

# 3D Numerical simulation of turbulent flow and heat transfer in a U-tube of different configurations

Khudheyer S. Mushatet<sup>1</sup>, Ayad Ali M<sup>2\*</sup>

<sup>1</sup>Mechanical Engineering Department, Engineering College, Thi-Qar University, Al-Nasiriya, Iraq

<sup>2</sup>Al-Furat Al-Awsat Technical University, Technical College/Al-Mussaib, Babil, Iraq

\*Corresponding author E-mail: [ayadial@yahoo.com](mailto:ayadial@yahoo.com)

## Abstract

In this work, three-dimensional incompressible turbulent flow and heat transfer in a tube of U-configuration has been investigated numerically. The influence using the U-tube in various cross-sectional shape, on thermal and hydrodynamic fields are presented in details. The cases of study for the U-tube are tested, by using the tube with different cross-sectional shapes (square and rectangle) and compare them with a circular cross-sectional shape, with a constant cross-sectional area and curvature radius ratio. The tube surface is subjected to a constant heat flux and the air is chosen to be the working fluid with turbulent flow under a range of Reynolds number (10000 to 25000). The turbulent flow and heat transfer is governed by continuity, momentum and energy equations. The effect of turbulence is treated by a k- $\epsilon$  turbulent model. ANSYS fluent code (15.0) based on finite volume method is used to get the numerical results. The flow separation and vortex formation at the bend section plays major role in heat and momentum transfer in bend tube. The obtained results of using of square and rectangular cross-sectional shape reduces the Nusselt number by 21.6% and 16.3% respectively as compared with the circular cross-section U-tube (the same circular cross-sectional area), and considerable decrease of the friction factor by 7.4% and 5.9% as compared with the circular cross-section U-tube. Numerical investigations indicated that within the circular cross-section U-tube a significant heat transfer enhancement is observed. In addition, the velocity fields for the primary and secondary flows were showed in a vector diagram. The present numerical results are compared with empirical correlations and verified a comparatively good agreement. The numerical method was validated by comparing the results with the experimental data and showed acceptable agreement.

**Keywords:** Turbulent; Heat Transfer; U-Tube; Numerical Investigation; Cross-Sectional Shape.

## 1. Introduction

U-tubes (two lengths of straight tube joined by 180° bend at one end) are commonly used in large engineering application, such as heat exchangers, gas turbine blades, waste heat reboilers, nuclear reactors, evaporators and steam generators e.g.

When a fluid moves through a straight tube, the fluid velocity near the centerline is higher than that near the wall. The effect is especially pronounced in laminar flow but is true for turbulent flow, too. When the tube is coiled or bent 180°, all fluid elements experience a centrifugal force radially outward which is proportional to the square of the element velocity and inversely proportional to the radius of the curvature. Therefore, the more rapidly moving elements near the centerline tend to move towards the outside, displacing the slower elements, which in turn move back toward the bend axis. The effect is to superimpose a "Secondary" flow pattern upon the primary flow.

Due to the existence of the secondary flow, the heat transfer is higher in a curved tube than in an equivalent straight tube under similar fluid flow conditions and the heat transfer mechanism is more complicated that's the reason of using numerical investigation. [1].

In the tube bend, due to local imbalance among pressure gradient and inertial forces, the flow is characterized as a secondary flow/circulation. It is mainly depend on the curvature of the pipe which is being a characteristic length of tube cross-section, for instance the radius or hydraulic radius, and the radius of curvature.

The characteristics of the secondary flow/circulation depend not only on Reynolds number and diameter, but also on the shape and size of the tube's cross-section. In developing flows, e.g. in the entrance region between a straight tube and a bend, they depend also on the distance from the curve entry

The study of turbulent flow and fluid behavior in U-tube configurations has been a subject of interest among many researches. Several researchers have examined the fluid flow and heat transfer characteristics experimentally as well as computationally.

Moshfeghian [2] studied the Heat transfer through a 180-bend tube. A Reynolds range from 7,300 to 27,000 was investigated for a bend radius of 9.875 inches and 7/8-inch OD (0.052-inch wall thickness). The test section was heated electrically by passing DC current through the tube wall. Analysis of the experimental data indicates that the local heat transfer coefficient in the straight section upstream of the bend is independent of peripheral position. The peripheral heat transfer is far from uniform in the bend, being much higher at the outside and lower at the inside of the bend, resulting in a higher mean heat transfer coefficient as compared to a straight tube under similar conditions. At any cross section in the bend, the distribution of peripheral heat transfer coefficient is almost symmetrical about a plane containing the longitudinal axis of tube and the radius of the bend. At the entrance region of the downstream section of the bend, the distribution of peripheral heat transfer coefficient is Symmetrical about the plane of the bend. In addition, the peripheral heat transfer coefficient is highest at the outside wall of the bend and lowest at the inside wall. Patel and Parekh[3] carried out the design of optimum size and the tempera-

ture difference of U – type shell and tube heat exchanger, general Design consideration and design procedure is also illustrated. Different types of methods are carried out for optimum design, by LMTD method,  $\epsilon$ -NTU method, P-NTU method and also for  $\Psi$ -NTU method, also According to design parameters experimental analysis is carried out. The results show that Keeping the hot water mass flow rate constant at 0.401kg/sec and varying cold water mass flow rate at 0.4785, 0.5173 and 0.5595 kg/sec, with increase in cold water temperature of 6.8°C, 5.7°C and 4.9°C respectively. Based on the design methodology, the shell and U tube heat exchanger designed and perform the experimental test. Sudo, et al.[4] An experimental steady, developing turbulent flow in a circular sectioned 180° bend has been investigated. The bend radius was (104 mm) and a curvature radius ratio ( $R_c$ ) was 4.0 with long, straight upstream and downstream pipes. The measurements of the radial, circumferential and longitudinal components of mean velocity, and corresponding components of the Reynolds stress were obtained with a hot wire anemometer at a Reynolds number of  $6 \times 10^4$  and at various longitudinal stations. It was shown that in the section upstream from a bend angle of about 60, both the flows through the 180° and the 90° bend are closely similar in their behavior. In the section from the bend angle of 90°, the high-velocity regions occurred near the upper and lower walls as a result of strong secondary flow and the turbulence with high level appears in the central region of the bend. Just after the bend exit, an further pair of vortices appears in the outside part of the cross section owing to the transverse pressure difference. In the downstream tangent, the flow returns slowly to the proper flow in a straight pipe, but it needs a longer distance for recovery than in the 90° bend. Janyanti et al [5] performed CFD analysis to examine the Gas-particle motion in 90° and 180° circular cross-section pipe bends. They found that the secondary flow induced in the gas phase due to curvature affects the motion of the particles which causes the smaller particles to come out of the bend without deposition. Clarke and Finn [6] studied the enhancement of internal convection heat transfer following a heat exchanger U-bend under laminar flow conditions. Numerical investigations, conducted using "FLUENT" computational fluid dynamics, to investigate the development of temperature profiles upstream of, within and downstream of a U-bend for a laminar flow refrigerant. The model geometry utilized in this study consisted of a U-bend preceded by a straight circular inlet pipe and followed by an identical straight circular outlet pipe. It was shown that centrifugally induced secondary flows, known as Dean Vortices, partially invert the temperature profile. It was found that Nusselt values downstream of a U-bend were found to exceed Nu values for a combined entry situation by greater than 20% for up to 20 pipe diameters downstream. Djebedjian et al. [7] investigated numerically the two-and three-dimensional incompressible turbulent flow through two types of square sectioned U-bend duct flows with mild and strong curvatures. Calculations were carried out using the flow analysis program FLUENT. Five turbulence models were implemented, namely: Standard k-  $\epsilon$  model, Renormalization-group (RNG) k-  $\epsilon$  model, Realizable k-  $\epsilon$  model, k-  $\epsilon$  model and Reynolds Stress Model (RSM). All models managed to mimic the general flow patterns and to predict a later separation position than the experiment. The reattachment lengths predicted by all models were over predicted. More advanced turbulence model such as the Reynolds stress model and RNG k- $\epsilon$  model had more reliable numerical results especially at separation zone. Nobari et al. [8] Analyzed three-dimensional incompressible viscous flow and heat transfer in a rotating U-shaped duct with a square cross-section. A numerical solution was used, the governing equations including full Navier–Stokes and energy equations are solved using a finite volume method based on the SIMPLER algorithm in an orthogonal uniform grid. Seven different major rotational directions were taken into account to study in detail the effects of rotational direction on the flow field pattern and consequently on the friction coefficient and heat transfer rate in a U-shaped duct, with a square cross-section considering isothermal boundary condition at the walls. The comparison of numerical results at different rotation

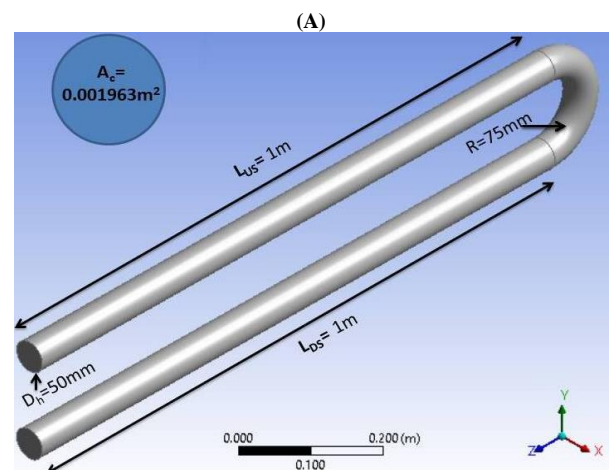
angles indicates that the maximum heat transfer rate occurs when the duct rotates about an axis parallel to the axis of duct curvature. Suga [9] predicted the turbulence and heat transfer in two types of square sectioned U-bend duct flows with mild and strong curvature, using recent second moment closures. A two-component limit turbulence model and the wall reflection free model were presented. The results presented that the two component limit turbulence model was dependable in the case of strong curvature. Azzola et al. [10] used Laser-Doppler velocimetry measurement to examine the turbulent flow in a 180 pipe bend. Numerical simulations have reproduced with an acceptable degree of conformity the measured evolution of the flow. Predictions of the flow development were presented based on a "semielliptic" truncation of the Reynolds equations in the main part of the flow with the standard k- $\epsilon$  effective viscosity model used to approximate the turbulent stress field. They found that the bend of angle between 90 and  $X/D = 5$  ( $X$  and  $D$  being the axial distance from the pipe inlet and pipe diameter respectively), the circumferential velocity profiles displayed secondary flow reversals which are independent of the Reynolds number.

The present investigation is undertaken to study the effect of a 180° bend on heat transfer to a single phase fluid in tubes and to obtain a better and more quantitative insight into the heat transfer process that occurs when a fluid flows in a U-bend tube, so the objectives of this study can be abbreviated as follows:

- Investigate the hydrodynamics and thermal performance of U-shaped tube.
- Testing the effect of changing the cross-section shape of U-tube on flow field, friction losses and heat transfer enhancement.

## 2. Model description

The physical domain consist of U-tube configuration, this configuration consists of three parts, i.e. the upstream tube, the U-bend and the downstream tube. The configuration consists of a square cross-sectional U-tube (SUT) and rectangular cross-sectional U-tube (RUT), with U-bend configuration and the same cross sectional area of the circular cross-sectional U-tube (CUT). The length of the upstream and the downstream of the tube is (1m), with curvature radius ratio " $R_c$ " equal to 1.5, as shown in Fig. 1.



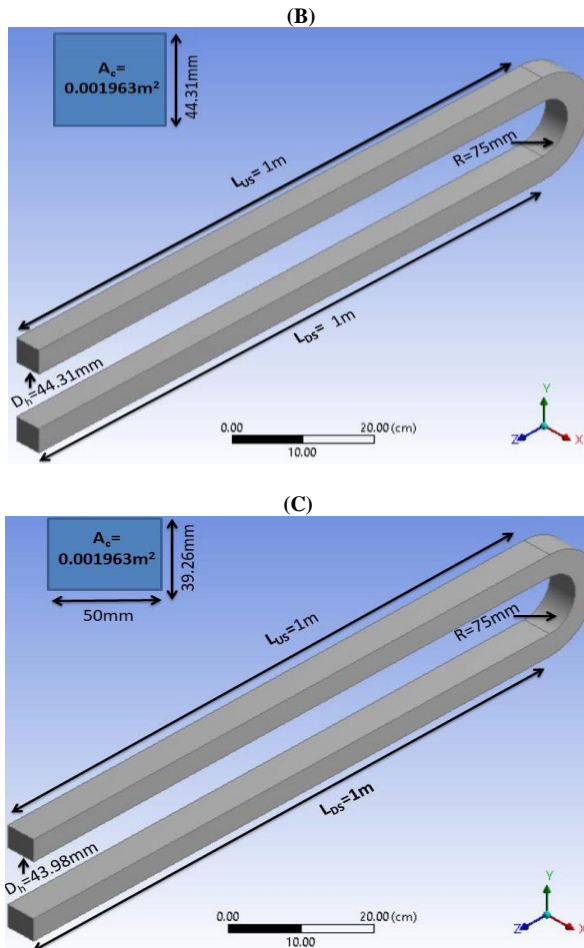


Fig. 1: The Geometry of the U-Bend Tube with Different Cross Sectional Area (A, B and C Is A Circular, Square and Rectangular U-Tube).

Air flows in the tube, enters with a different velocities and the outlet is assumed to be an outflow boundary. Turbulent, isothermal, and steady state conditions will be considered to solve the flow field. The study has covered four Reynolds numbers from 10000 to 25000 and a constant Prandtl number. Local heat transfer coefficients were computed from knowledge of local heat flux values along the test section which is  $1000 \text{ w/m}^2$

### 3. Mathematical model and numerical analysis

#### 3.1. Assumptions

The following assumptions are used to simplify the proposed model solution:

- 1) The fluid is air.
- 2) The fluid has constant properties.
- 3) Steady state flow.
- 4) Incompressible flow.
- 5) The gravity effect is neglected.
- 6) Non-slip flow is assumed.
- 7) The dissipation of heat is assumed to be neglected.
- 8) Negligible wall thickness.

#### 3.2. Governing equations for the turbulent flow

The description of the fluid motion in the tube for the turbulent state is made by solving the average differential equation of mass (continuity) and momentum equation in addition to the (k- $\epsilon$ ) model equation. The turbulent flow is characterized by fluctuation velocity field.

In describing the turbulence flow in mathematical terms, it's convenient to separate it into mean motion and a fluctuation or eddy motion. As in the following form:

#### 3.2.1. Continuity Equation:

$$\frac{\partial u}{\partial x} + \frac{\partial v}{\partial y} + \frac{\partial w}{\partial z} = 0 \quad (1)$$

Continuity equation is a mathematical representation for the mass conservation. Its form is [11]:

#### 3.2.2. Momentum equations (NSES)

Momentum equation in x-direction:

$$\rho \left( \frac{\partial u^2}{\partial x} + \frac{\partial uv}{\partial y} + \frac{\partial uw}{\partial z} \right) = -\frac{\partial p}{\partial x} + \frac{\partial}{\partial x} \left( 2\mu_{\text{eff}} \frac{\partial u}{\partial x} \right) + \frac{\partial}{\partial y} \left( \mu_{\text{eff}} \frac{\partial u}{\partial y} \right) + \frac{\partial}{\partial z} \left( \mu_{\text{eff}} \frac{\partial u}{\partial z} \right) \quad (2)$$

Momentum equation in y-direction:

$$\rho \left( \frac{\partial vu}{\partial x} + \frac{\partial v^2}{\partial y} + \frac{\partial vw}{\partial z} \right) = -\frac{\partial p}{\partial y} + \frac{\partial}{\partial x} \left( \mu_{\text{eff}} \frac{\partial v}{\partial x} \right) + \frac{\partial}{\partial y} \left( 2\mu_{\text{eff}} \frac{\partial v}{\partial y} \right) + \frac{\partial}{\partial z} \left( \mu_{\text{eff}} \frac{\partial v}{\partial z} \right) + \frac{\partial}{\partial x} \left( \mu_{\text{eff}} \frac{\partial v}{\partial y} \right) + \frac{\partial}{\partial y} \left( \mu_{\text{eff}} \frac{\partial v}{\partial x} \right) + \frac{\partial}{\partial z} \left( \mu_{\text{eff}} \frac{\partial v}{\partial y} \right) \quad (3)$$

Momentum equation in z-direction:

$$\rho \left( \frac{\partial wu}{\partial x} + \frac{\partial wv}{\partial y} + \frac{\partial w^2}{\partial z} \right) = -\frac{\partial p}{\partial z} + \frac{\partial}{\partial x} \left( \mu_{\text{eff}} \frac{\partial w}{\partial x} \right) + \frac{\partial}{\partial y} \left( \mu_{\text{eff}} \frac{\partial w}{\partial y} \right) + \frac{\partial}{\partial z} \left( 2\mu_{\text{eff}} \frac{\partial w}{\partial z} \right) + \frac{\partial}{\partial x} \left( \mu_{\text{eff}} \frac{\partial w}{\partial z} \right) + \frac{\partial}{\partial y} \left( \mu_{\text{eff}} \frac{\partial w}{\partial z} \right) \quad (4)$$

Where  $\mu_t$  is the eddy, or turbulent, viscosity.

In turbulent flow governing equations, the terms of turbulent stresses are added to the terms of laminar stresses using the concept of effective viscosity.

$$\mu_{\text{eff}} = \mu + \mu_t \quad (5)$$

#### 3.2.3. Energy equation

$$\frac{\partial uT}{\partial x} + \frac{\partial vT}{\partial y} + \frac{\partial wT}{\partial z} = \frac{\partial}{\partial x} \left( \Gamma_{\text{eff}} \frac{\partial T}{\partial x} \right) + \frac{\partial}{\partial y} \left( \Gamma_{\text{eff}} \frac{\partial T}{\partial y} \right) + \frac{\partial}{\partial z} \left( \Gamma_{\text{eff}} \frac{\partial T}{\partial z} \right) \quad (6)$$

### 3.3. The standard k- $\epsilon$ model

The standard k- $\epsilon$  model has two model equations one for k and one for  $\epsilon$ . The model transport equation for k is derived from the exact equation, while the model transports equation for  $\epsilon$  was obtained by using the physical analysis. The standard model uses the following transport equations for k and  $\epsilon$ .

For turbulent kinetic energy (k):

$$\rho \left( \frac{\partial}{\partial x} (ku) + \frac{\partial}{\partial y} (kv) + \frac{\partial}{\partial z} (kw) \right) = \frac{\partial}{\partial x} \left( \frac{\mu_t}{\sigma_k} \frac{\partial k}{\partial x} \right) + \frac{\partial}{\partial y} \left( \frac{\mu_t}{\sigma_k} \frac{\partial k}{\partial y} \right) + \frac{\partial}{\partial z} \left( \frac{\mu_t}{\sigma_k} \frac{\partial k}{\partial z} \right) + G - \rho \epsilon \quad (7)$$

For energy dissipation rate ( $\epsilon$ ):

$$\rho \left( \frac{\partial}{\partial x} (\epsilon u) + \frac{\partial}{\partial y} (\epsilon v) + \frac{\partial}{\partial z} (\epsilon w) \right) = \frac{\partial}{\partial x} \left( \frac{\mu_t}{\sigma_\epsilon} \frac{\partial \epsilon}{\partial x} \right) + \frac{\partial}{\partial y} \left( \frac{\mu_t}{\sigma_\epsilon} \frac{\partial \epsilon}{\partial y} \right) + \frac{\partial}{\partial z} \left( \frac{\mu_t}{\sigma_\epsilon} \frac{\partial \epsilon}{\partial z} \right) + C_{1\epsilon} \rho \frac{\epsilon}{k} G - C_{2\epsilon} \rho \frac{\epsilon^2}{k} \quad (8)$$

Where G is referred to the generation term and is given [12]:

$$G = \mu_t \left[ 2 \left( \frac{\partial u}{\partial x} \right)^2 + 2 \left( \frac{\partial v}{\partial y} \right)^2 + 2 \left( \frac{\partial w}{\partial z} \right)^2 + \left( \frac{\partial v}{\partial y} \frac{\partial u}{\partial x} \right)^2 + \left( \frac{\partial v}{\partial z} \frac{\partial w}{\partial x} \right)^2 + \left( \frac{\partial w}{\partial z} \frac{\partial v}{\partial y} \right)^2 \right] \quad (9)$$

Also,

$$k = \frac{1}{2} (\overline{u'^2} + \overline{v'^2} + \overline{w'^2}) \quad (10)$$

$$\varepsilon = \overline{e'_{ij} e'_{ij}} \quad (11)$$

The turbulent kinetic energy (k) and the dissipation rate of the turbulent kinetic energy ( $\varepsilon$ ) are chosen as the two properties to determine the turbulent viscosity ( $\mu_t$ ). Where

$$\mu_t = \rho c_\mu \frac{k^2}{\varepsilon} \quad (12)$$

Where:  $c_\mu$  is a constant.

### 3.4. Boundary conditions

The boundary conditions are specified for each zone of the computational domain as follow :

- 1) Inlet boundary conditions
  - a) Uniform inlet velocity,  $U=U_{in}$ .
  - b) The flow is isothermal ( $T=T_{in}=300K$ ).
- 2) Wall Boundary Condition
  - a) The velocity at the walls is taken to be zero (no slip). ( $u=v=w=0$ ) in the x, y and z direction.
  - b) A constant heat flux ( $q=1000W/m^2$ ).
- i) Concentrated overall surface area of the wall in the circular cross-section tube.
- ii) Concentrated on the inner surface area of the wall in the square and rectangular tube.
- 3) Outlet Boundary Condition
  - a) Zero gage pressure is specified at the outlet domain .

### 3.5. Hydrodynamic parameters

In this section, signification parameters are defined as below:

- 1) The Reynolds number:

$$Re = \rho U_{in} D_h / \mu \quad (13)$$

Where  $D_h$  is the hydraulic diameter.

- 2) Friction coefficient

The friction coefficient can be expressed in shear stress at the tube surface is defined as:

$$C_f = \tau_w / \frac{1}{2} \rho U^2 \quad (14)$$

Where  $\tau_w$  is the wall shear stress and defined as:

$$\tau_w = \mu \sqrt{\left(\frac{\partial u}{\partial y}\right)^2 + \left(\frac{\partial w}{\partial y}\right)^2} \quad (15)$$

For the turbulent flow and due to complex behave of this flow the friction factor always calculates from the experimental equations. Therefore, for the turbulent flow  $Re \leq 2 \times 10^4$  friction factor is given by [13]:

$$f = 0.316 Re_{D_h}^{-1/4} \quad (16)$$

In addition, friction coefficient (Fanning fraction factor) is given by [13]:

$$c_f = \frac{f}{4} \quad (17)$$

- 3) The bulk temperature:

$$T_b = \frac{\int \rho T_i \rho dV_i}{\int \rho dV_i} = \frac{\sum_{i=1}^n T_i \rho |V_i|}{\sum_{i=1}^n \rho |V_i|} \quad (18)$$

- 4) The wall temperature: The wall temperature is described as:

$$T_w = \frac{1}{A} \int T_i dA_i = \frac{1}{A} \sum_{i=1}^n T_i |A_i| \quad (19)$$

- 5) The pressure drop

The pressure drop is described as:  $\Delta P = P_{in} - P_{out}$  (20)

$P_{in}$  was calculated by surface integral by means of area weighted average:

$$P = \frac{1}{A} \int P_{in} dA_{in} \quad (21)$$

- 6) The coefficient of heat transfer is defined as:

$$h = \frac{q''}{T_w - T_b} \quad (22)$$

- 7) The Nusselt number: The Nusselt number is defined as:

$$Nu = \frac{h D_h}{K} \quad (23)$$

### 3.6. Numerical analysis

Computational Fluid Dynamics (CFD) is considered the science that helps the computers to produce quantitative calculation of fluid flow basis. This includes the governing fluid motion and conservation laws, and considered the tools basis to design and develops the engineering application .(CFD) is become necessary work of many researchers in the world because it used predict internal flow and the development of computer became accurate and near to the fact. FLUENT program is used in advanced numerical applications to solve many problems in order to achieve effective results for many different models.

#### 3.6.1. Grid independency

A grid independence study is made to choose the optimum grid to get a better solution. The present results consider three different value for the grid independency investigate. The results are summarized in Table 1 show the specified grid for all shapes. The Nusselt number is determined for all shapes at  $Re = 10000$ . It is found that there is a small change in the average value of Nusselt number. The grid resolution investigation reveal that CUT, SUT and RUT become independent of the grid at cells, 1,197,774 , 1,199,266 and 1,142,400 cells respectively.

**Table 1:** Different Grids and Their Nusselt Number and Friction Factor Results for Different Studied Cases

No.	Case	No. of grid elements	Nu	Nu deviation	f	f deviation
1	CUT	1,008,000	40.05469	0.011956	0.037385	0.028532
		1,197,774	40.53936	0.021926	0.038483	0.025722
		1,480,347	41.44816		0.039499	
2	SUT	1,008,000	33.708	0.002973	0.032385	0.036992
		1,199,266	33.8085	0.008694	0.033629	0.148611
		1,480,347	34.105		0.039499	
3	RUT	1,008,000	34.302	0.004437	0.032385	0.054176
		1,142,400	34.45486	0.010003	0.03424	0.133143
		1,480,347	34.803		0.039499	

#### 3.6.2. Solving by fluent

The numerical method of discretized governing equations can be solved by writing a code or the problem can be solved by using one of the commercial (CFD) code. ANSYS FLUENT 15.0 software is used to calculate the current numerical investigation, Since Fluent is generally used in this field and it is considered one of the greater among other available codes. With a RNG (k- $\varepsilon$ ) model, a finite volume discretization is used in approximating the governing equations. A double-precision and pressure-based solver is used in the numerical computation. A non-slip boundary condition is adopted on pipe surface. The SIMPLE algorithm is used for pressure-velocity coupling. A second-order upwind scheme was adopted to the discretization of all terms.

### 4. Results and discussion

In this section, the numerical results has been addressed to verify the intensification of forced convection in a U-tube configuration with different shapes. The hydraulic diameter of the U-tubes is (0.05m, 0.04431m and 0.04398m) for the circular, square and rectangular cross-section, respectively. The studied cases for U-tube with different cross section shape (square, rectangular) with the same cross sectional area of the circular cross-sectional U-tube are discussed.

The effect of the cross section shape on the average Nusselt number variation for different values of Reynolds number is described in Fig. 2. It is noticed that the Nusselt number increases as the Reynolds number increases for all cross section shape due to the growths in fluid turbulence. Higher turbulence increases the intensity of secondary flow and hence the Nusselt number. The highest Nusselt number values indicated for the rectangular cross-section shape as compared with the square cross sectional U-tube. The results verified that the enhancement in the mean Nusselt is found to be 16.3% and 21.6% for the circular cross section U-tube as compared with the rectangular and square cross sectional U-tube, respectively. The circular tube gives the most heat transfer for the least pressure drop, which explains the overwhelming popularity of circular tubes in heat transfer equipment [14].

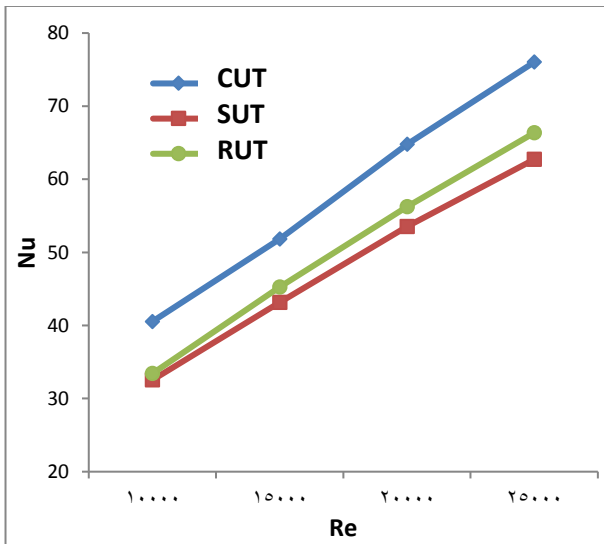


Fig. 2: Effect of Cross Section Shape on Nusselt Number for U-Tube.

Fig. 3. shows the influence of the cross section shape on the average friction factor variation for different values of Reynolds number. It can be noticed that the friction factor acquired from the square and rectangular cross-section shapes are reduces with increasing Reynolds number. It is viewed from the figure that there is reduction in the friction factor for utilizing rectangular and square cross sectional U-tube, and there is a significant rise in the friction factor for circular cross section U-tube, for the same cross sectional area. The gained results indicated that the increase in the friction factor is found to be 5.9% and 7.4% for circular cross section, as compared with the rectangular and square cross sectional U-tube. It can be observed that use of the U-bend configuration lead to greater friction factor for all the considered cross section shapes. This is because of the high wall shear stress at the bend section.

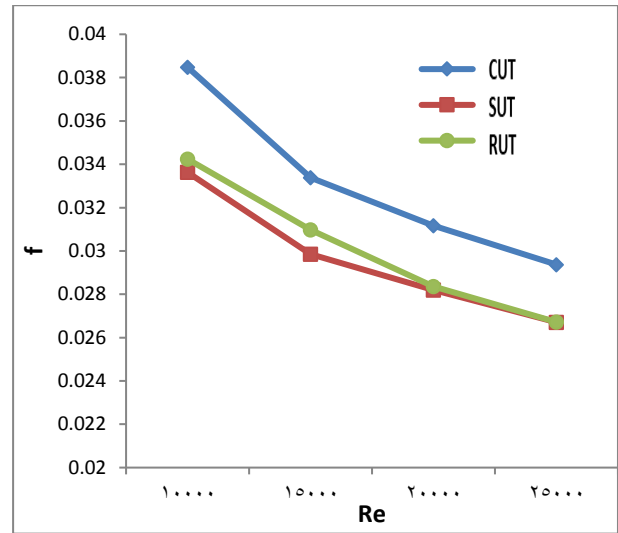


Fig. 3: Effect of Cross Section Shape on Friction Factor Variation for U-Tube.

The influence of the cross section shape on the pressure drop variation for different values of Reynolds number is depicted in Fig. 4. It can be examined that the pressure losses obtained from using square and rectangular cross-section shapes are increased with the increase of Reynolds number. The circular cross section U-tube denoted the highest growth in pressure drop as contrasted with the square and rectangular U- tubes. The collected results illustrated a growth in the pressure loss is found to be 5.86% and 7.8% for circular cross section U-tube, as compared with the rectangular and square cross-sectional U-tube. The presence of secondary flow dissipates kinetic energy, thus increasing the resistance to flow, which is agreed with [36]. Using the U-bend configuration clearly raises the pressure loss, this is because of the high produce of the reverse flow, and due to the length of the U-tube which is greater than of the straight tube.

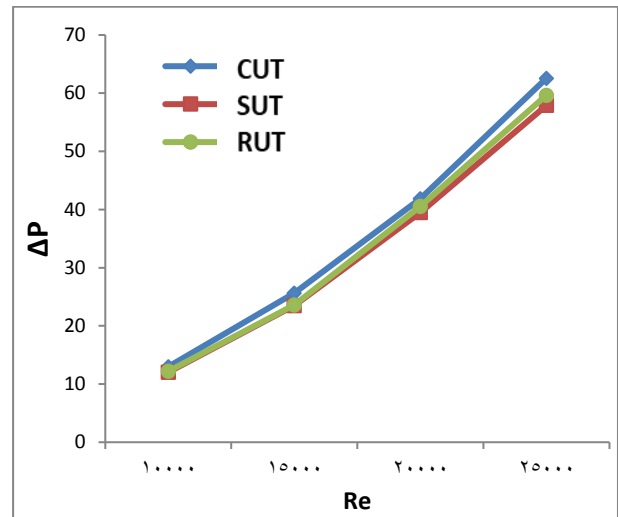
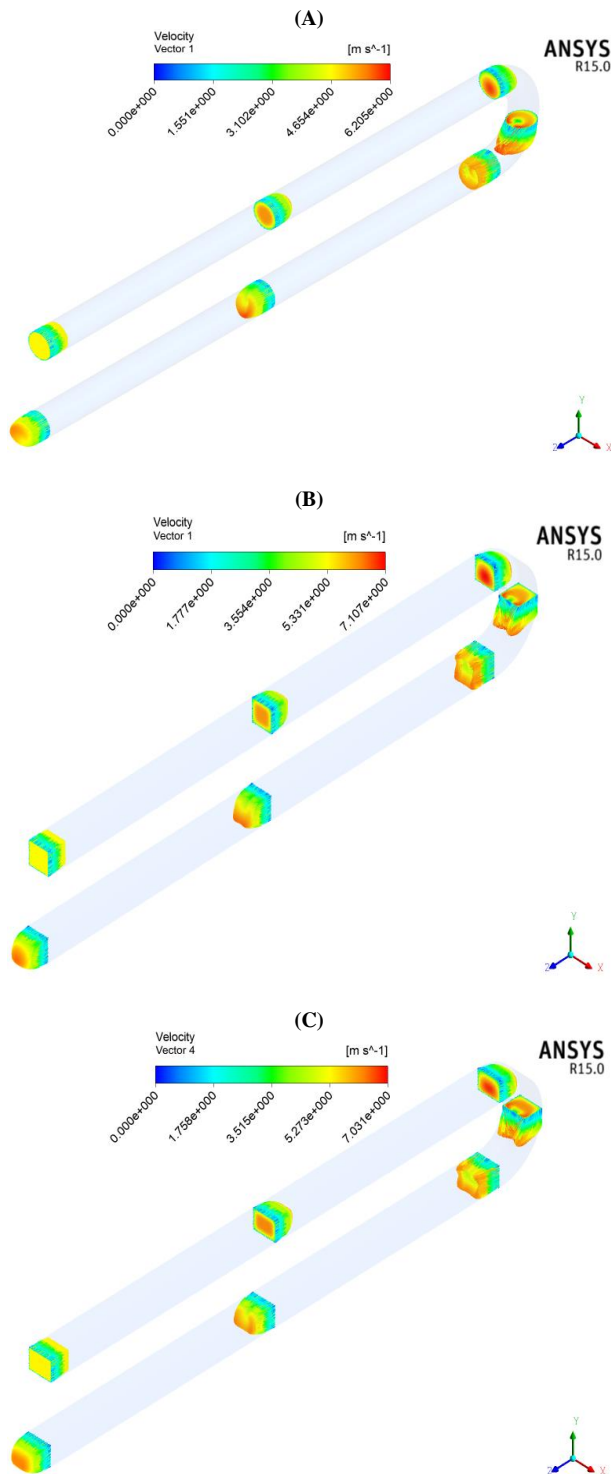


Fig. 4: Effect of Cross Section Shape on Pressure Drop Variation for U-Tube.

The gotten numerical results in present work for flow inside heated U-tube configuration with different arrangements cross sectional shapes will examined along this section to present realization about the flow and thermal attitude affecting. Fig. 5 presents the velocity vectors for the case of U-tube and the effect of the cross-section shape variation, for air flowing with Re = 15000. For all cross sectional shapes the velocity of flow in upstream tube domain will rise by going away from the tube wall toward its center reached its highest value at the center, the frame a, b and c illustrates the velocity vectors for the circular, square and rectangular U-tube, respectively.

When the fluid enters the U-bend area the tangential velocity rises and eddy flow is produced, for the current model, at 90° through the bend, the maximum transverse velocity was approximately 6.04m/s, 6.77m/s and 6.59m/s for the circular, square and rectangular U-tube, respectively



**Fig. 5:** Velocity Vector for U- Tube for Re=15000 of Different Cross Section Shape (A, B and C Is the Circular, Square and Rectangular U-Tube).

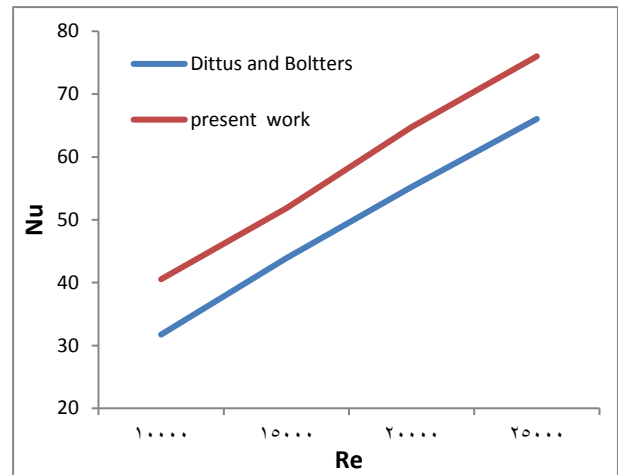
**4.1. The comparison between the numerical work and published results**

The collected numerical results are validated with existing empirical correlations for Nusselt number and friction factor. Before the primary analysis, Nusselt numbers for the U-tube are calculated under a consistent heat flux condition and then contrasted with those acquired from the essential Eq. (24) by Dittus and Boelter.

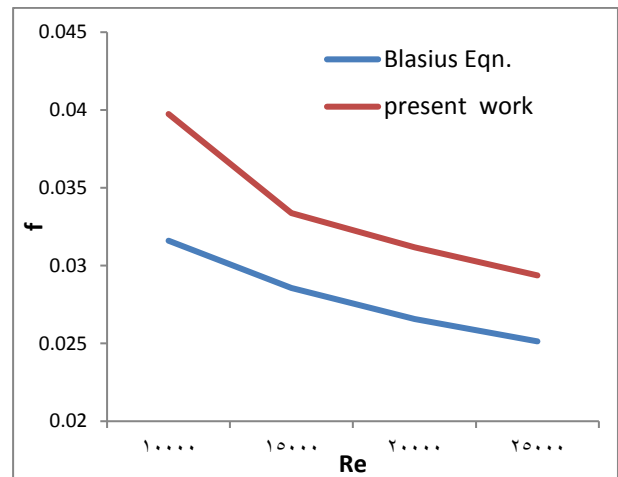
$$Nu = 0.023Re^{0.8}pr^{0.4} \tag{24}$$

Fig.6 exposes that the heat transfer results of the present work for the cross-section U-tube (CUT) agree appropriately with those acquired from Eq. (24) with the differences of less than ± 21.7%. The variations of friction factor with Reynolds number for the existing plain tube are offered in Fig. 7. It is realized that the friction factors are within ± 20% as contrasted to those accomplished from Blasius correlation.

$$f = 0.316 Re^{-0.25} \tag{25}$$



**Fig. 6:** Validation the Present Results of Average Nusselt Number with Dittus and Boltters for CUT.



**Fig. 7:** Validation the Present Results of Average Friction Factor with Blasius for CUT.

**4.2. Validations**

The results of friction factor for U-tube found through this work numerically for the experimental works of [15].The validations includes the friction factor as displayed in Fig. 8. The average deviation for average friction factor between the experimental works of [15] and the theoretical works is 14% and between the Blasius equation for [15] and the theoretical works is 27%.

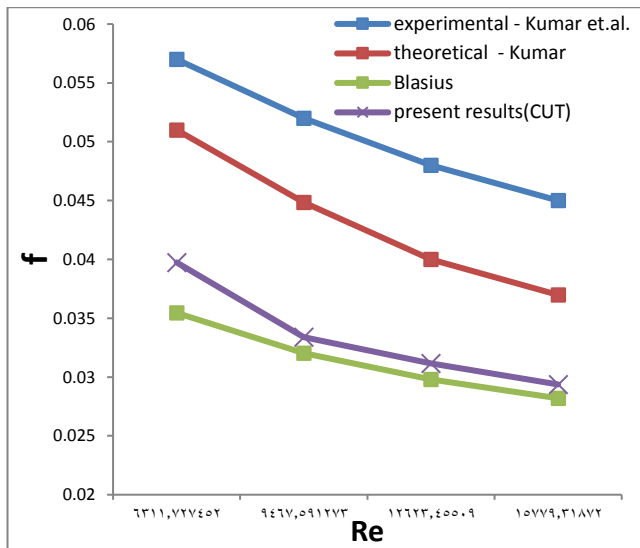


Fig. 8: Validation of the Theoretical Works with Results of [15] and Blasius Equation for Circular Cross Section U-Tube.

## 5. Conclusions

- 1) The heat transfer in the tube could be augmented highly by using U-bend configuration.
- 2) The utilization of the circular cross-section shape offers superior heat transfer than that of the square and rectangular cross-sectional shape arrangements.
- 3) Over a range of studied Reynolds numbers, rectangular cross-section shape yielded higher Nusselt number, enhancement efficiency and friction factor in comparison with the square shape of the same cross-sectional area.
- 4) Empirical relations for the Nusselt number and friction factor are presented for a comparison use.
- 5) The fluid circulation in the U-bend area for utilizing for the square cross-sectional shape increases the fluid circulation in the U-bend area as compared with the rectangular cross-section and the circular cross-section U-tube, for the same cross-sectional area and Reynolds number equal to 15000.

## References

- [1] Mahmood M., 'fluid flow and heat transfer in u-bends', PhD thesis, Oklahoma State University, USA(1978)
- [2] Mahmood M., 'The effect of a 180° bend on turbulent heat transfer coefficient in a pipe', M.Sc thesis, Oklahoma State University, USA (1975).
- [3] Divyesh B. Patel, Jayesh R. Parekh, 'Design and experimental analysis of shell and tube heat Exchanger (U-Tube)', International journal of advanced research in engineering, science & management, 1 (5), pp.1-8, (2015).
- [4] Sudo K, Sumida M, Hibara H, Experimental investigation on turbulent flow through a circular-sectioned 180° bend', Experiments in Fluids, Vol. 28(1), pp. 51–57, (2000). <https://doi.org/10.1007/s003480050007>.
- [5] Jayanti S, Wang M, Mayinger F., Gas-particle flow through bends. IMechE C461; 24:pp. 161-166, (1993).
- [6] Clarke R, and Finn D, Numerical investigation of the influence of heat exchanger U-Bends on temperature profile and heat transfer of secondary working fluids, Proceedings of the 5th European Thermal-Sciences Conference, The Netherlands, (2008).
- [7] Djebedjian, B, Mohamed, M., and Elsayed, A., "Numerical studies of curvature effect on turbulent flows in 180° curved ducts," Proceedings of IEC 2008, 6th International Engineering Conference, Mansoura/Sharm El-Sheikh, Egypt, 20-23 March, Vol. 2, pp.347-370, (2008).
- [8] Nobari, M, Nousha A, Damangir E, A numerical investigation of flow and heat transfer in rotating U-shaped square ducts', International Journal of Thermal Sciences, Vol. 48, pp. 590–601, (2009). <https://doi.org/10.1016/j.ijthermalsci.2008.04.001>.

- [9] Suga K, Predicting turbulence and heat transfer in 3-D curved ducts by near-wall second moment closers. International Journal of Heat Mass Transfer; 46:161–73, (2003). [https://doi.org/10.1016/S0017-9310\(02\)00249-1](https://doi.org/10.1016/S0017-9310(02)00249-1).
- [10] Azzola J, Humphrey JAC, Lacovides H, Launder BE, Developing turbulent flow in a U-bend of circular cross-section: measurement and computation. Journal of Fluids Engineering, Vol.108, pp. 214-221, (1986). <https://doi.org/10.1115/1.3242565>.
- [11] Streeter V and Wylie E, Fluid mechanics, First SI Metric Edition, fifth printing, ISBN: 0-07-548015-8.
- [12] Mahdi, H, Numerical and experimental study of enhancement of heat transfer in roughened ribbed Duct, PhD thesis, Department of technical Education, University of technology, Iraq, (2004).
- [13] Saysroy A, Eiamsa-ard S, Enhancing convective heat transfer in laminar and turbulent flow regions using multi-channel twisted tape inserts. International Journal of Thermal Sciences, Vol. 121, pp.55-74, (2017). <https://doi.org/10.1016/j.ijthermalsci.2017.07.002>.
- [14] Yunus A. , Afshin J, Heat and mass transfer: fundamentals and applications, Fifth Edition, McGraw-Hill Education, 2 Penn Plaza, New York, NY,2015.
- [15] Priyanka B, Manish J, and Anirudh G., Comparison of heat transfer between a circular and rectangular tube heat exchanger by using Ansys Fluent, International Journal of Thermal Technologies, Vol.4, No.2, (2014).